# Atomic Structure of the $\alpha$-$Al_2O_3(0001)$ $(\sqrt{31} \times \sqrt{31})R \pm 9°$ Reconstruction

G. Renaud,[1,2] B. Villette,[1,2] I. Vilfan,[3] and A. Bourret[1]

[1]*Commissariat à l'Energie Atomique, Département de Recherche Fondamentale sur la Matière Condensée, SP2M, 85X, 38041 Grenoble Cedex, France*

[2]*Laboratoire pour l'Utilisation du Rayonnement Electromagnétique, 91405 Orsay Cedex, France*

[3]*J. Stefan Institute, PO Box 100, SI-61111 Ljubljana, Slovenia*

(Received 27 October 1993)

The projected atomic structure of the $\alpha$-$Al_2O_3(0001)(\sqrt{31} \times \sqrt{31})R \pm 9°$ reconstruction has been analyzed by means of the grazing incidence x-ray diffraction technique, which is not limited by the surface insulating character. It consists of two Al planes whose structure is close to that of metallic Al(111). This overlayer is rotationally reconstructed, is commensurate with the substrate, and displays strong nonlinear static distortion waves. This layer, oxygen depleted, explains why the surface properties are dramatically changed.

PACS numbers: 68.35 Bs, 61.10.–i, 81.60.Dq

The structure, composition, and morphology of ceramic surfaces strongly influence their chemical, mechanical, and electrical properties, and play a major role in many technologically important processes such as corrosion, catalysis, and sintering. They also affect the nature and strength of bonding at metal/ceramic interfaces used in composites or in electronic packaging. The (0001) surface of sapphire is of major importance; it is used as a substrate in silicon on sapphire technology and in growth of several materials, such as high-temperature superconductors, large-gap semiconductors, and refractory metals. Its initial state is known to play a dominant role on the overlayer properties. While theoretical investigations concentrate on the unreconstructed surface structure and energy and its bonding with metals [1–3], current experimental research is devoted to conditioning the $\alpha$-$Al_2O_3(0001)$ surface by various heat treatments [4–6] in order to improve the quality of the interface. When heated to high temperature under vacuum, several reconstructions appear: $(\sqrt{3} \times \sqrt{3})R30°$, $(3\sqrt{3} \times 3\sqrt{3})R30°$, and finally $(\sqrt{31} \times \sqrt{31})R \pm 9°$. Although their electronic structure and symmetry are now well characterized [4–6], their atomic structure remains essentially unknown, mainly because of the difficulty to characterize insulators with standard UHV tools such as low energy electron diffraction (LEED) or scanning tunneling microscopy. The $(\sqrt{31} \times \sqrt{31})R \pm 9°$ reconstruction is of particular interest because it has been reported to help epitaxy and enhance adhesion in some cases [7]. Moreover, it is unusually stable even under non-UHV conditions, i.e., after air exposure. A structural model for this reconstruction was proposed more than two decades ago [4]. The LEED pattern was interpreted as the superposition of two reciprocal lattices, that of the hexagonal substrate and that of a nearly cubic overlayer with composition $Al_2O$ or AlO, plus the interference pattern because of double diffraction. However, this model remained controversial. In particular, this interpretation does not include a supercell formation with atomic relaxations.

The aim of the present study is to analyze the $\alpha$-$Al_2O_3(0001)(\sqrt{31} \times \sqrt{31})R \pm 9°$ reconstruction in order to get unambiguous answers concerning the presence of a supercell, and ultimately to determine its atomic structure. We used grazing incidence x-ray diffraction (GIXD) [8], which does not suffer the limitations (charging and multiple scattering effects) of electron based techniques.

The $\alpha$-$Al_2O_3(0001)$ single crystals were first annealed in air at 1500 °C for 3 h. This annealing restores the surface stoichiometry and crystallinity and yields a surface with atomically flat, ~1000 Å wide terraces, separated by monolayer or bilayer high steps [9], as confirmed on our samples by atomic force microscopy investigations in air. The samples were then heated to ~1350 °C for ~20 min in UHV to obtain the $\sqrt{31}$ reconstruction. No impurity could be detected by x-ray photoelectron spectroscopy (XPS) after this treatment. GIXD and LEED, performed on several samples, showed that with the above explained preparation conditions, there is a reproducible final reconstruction state, with a well-defined, stable atomic structure. The samples were exposed for a short time (~10 min) to ultradry nitrogen during transfer between the preparation and the GIXD chambers.

The GIXD measurements were performed with a new surface diffraction setup developed on the W21 wiggler beam line of the DCI synchrotron storage ring of LURE (Laboratoire pour l'Utilisation du Rayonnement Electromagnétique, Orsay, France), which delivers a beam focused both vertically and horizontally. The wavelength was set to 1.0403 Å, the incident angle fixed at the critical angle for total external reflection, $\alpha_c = 0.21°$, and the pressure maintained to $\sim 1 \times 10^{-9}$ Torr during the experiment.

The reconstruction diffraction rods were examined at the ideal locations for a perfectly commensurate reconstruction with the following relations to the substrate, deduced from the LEED pattern:

$$\mathbf{a}_S^* = \frac{1}{31}(5\mathbf{a}_B^* + \mathbf{b}_B^*) \quad \text{and} \quad \mathbf{b}_S^* = \frac{1}{31}(-\mathbf{a}_B^* + 6\mathbf{b}_B^*),$$

  

where $(\mathbf{a}_B^*, \mathbf{b}_B^*)$ and $(\mathbf{a}_S^*, \mathbf{b}_S^*)$ are, respectively, the in-plane reciprocal unit vectors of the hexagonal bulk unit cell and of the hexagonal $(\sqrt{31} \times \sqrt{31})R = +\arctan(\sqrt{3}/11)$ reconstruction. A large number, 366 of which 267 were inequivalent, of in-plane reflections arising from the reconstruction alone (excluding those on the bulk reciprocal lattice) were measured under grazing incident and exit angles (at $\ell = 0.12$ in units of $c^* = 2\pi/12.991$ Å$^{-1}$) by performing rocking scans. All peaks were exactly centered at the expected positions to within 0.001° of azimuthal rotation, which shows that the surface reconstruction is perfectly *commensurate* with the underlying bulk lattice. Their width and Lorentzian shape indicate an exponential decay in correlations with the decay length of ~500 Å. Several reconstruction diffraction rods were also measured up to out-of-plane momentum transfer magnitude of 3 Å$^{-1}$. The absence of symmetry of the intensity with respect to $\ell = 0$ shows that the reconstruction has the minimal hexagonal symmetry $p3$.

The experimental diffraction pattern (Fig. 1), obtained after integration of the rocking scans and correction for polarization, Lorentz, and viewed-area factors, has sixfold symmetry, with 7% reproducibility between equivalent reflections. An important result is that measurable intensity is found at *all* reciprocal lattice points of the *reconstructed unit cell,* even far away from bulk Bragg peaks. Because x-ray scattering by surfaces is by essence kinematical, this result contradicts previous interpretations of the LEED pattern [4] in terms of multiple electron scattering due to the coincidence of lattice sites between a rearranged surface layer with a small unit cell and the hexagonal substrate. In that case, x-ray diffraction peaks other than bulk would be found *only* at the reciprocal lattice points of the *surface* and *bulk* unit cells. The x-ray diffraction intensity distribution proves that there indeed is a genuine $(\sqrt{31} \times \sqrt{31})R \pm 9°$ supercell formation with atomic relaxations.

The diffraction pattern is qualitatively very similar to that predicted [10,11] in the case of *rotational epitaxy* of an hexagonal overlayer, which is expanded and rotated with respect to an ideal overlayer $R$ in perfect registry. The main peaks (hatched in Fig. 1) correspond to the first-order approximation, called "parent" phase, of the adsorbed structure. Their locations yield the expansion, 10.62%, and rotation, 2.361°, applied to the $R$ phase to obtain this rigid hexagonal parent phase. The other diffraction peaks are satellites corresponding to the static distortions of this parent phase and possibly to additional disorder. Figure 3 shows the corresponding parent phase, composed of two perfect Al(111) planes (as will be shown below) which are just rotated and expanded with respect to the substrate, and are commensurate, with a $(\sqrt{31} \times \sqrt{31})R \pm 9°$ coincidence site lattice (CSL).

Figure 4 shows the experimental pair-correlation (Patterson) function. Most Patterson peaks have a nearly perfect hexagonal arrangement. The positions of these peaks can be directly constructed by a rotation of ~1.4° followed by a small expansion of the projected atomic positions of an fcc (111) (*A-B-C*) stacking on top of the oxygen hcp (0001) (*A-B-A-B*) stacking of the underlying bulk lattice. The Patterson superposition method shows that these hexagonally ordered peaks correspond to existing atomic positions within the reconstructed unit cell or within its variant [12]. In projection, the reconstruction consists of *domains* of one or more close-packed planes separated by *domain walls.* Different initial structures were systematically studied. All structures based on fcc or hcp stacking of either 1, 2, 3, or 4 planes made either of Al or O atoms and with different locations of the origin of the unit cell were tested. Further quantitative analysis consists in least-squares refinement of all in-

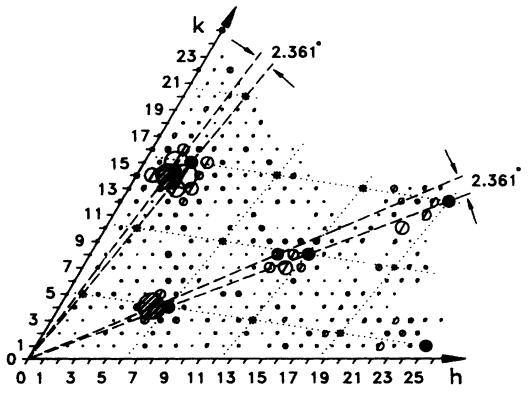


FIG. 1. Experimental diffraction pattern, indexed in the reciprocal space of the reconstructed unit cell (in $\frac{1}{6}$ of the $\ell = 0.12$ reciprocal plane). The radii of the right-hand halves of the open circles are proportional to the experimental structure factors, while the left-hand open circles are calculated from the best model ($\chi^2 = 1.2$). Black disks represent bulk allowed and CTR reflections. The bulk unit mesh is superposed as dotted lines. The three main diffraction peaks of the reconstruction, corresponding to the parent phase, are hatched.

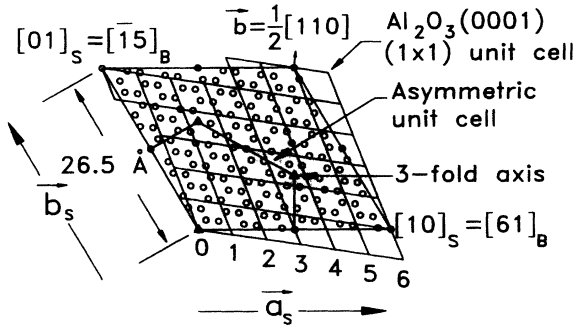


FIG. 2. The $(\sqrt{31} \times \sqrt{31})R9°$ unit cell, with positioning of the threefold axes, the asymmetric unit cell, and its relationship to the bulk unit cell (hexagonal mesh). The atomic positions of the two perfect Al(111) planes of the parent phase are shown. This parent phase analysis allows one to assign a Burgers vector to the domain walls, which is $\frac{1}{2}\langle 110\rangle$ in the ideal Al(111)$R$ lattice.

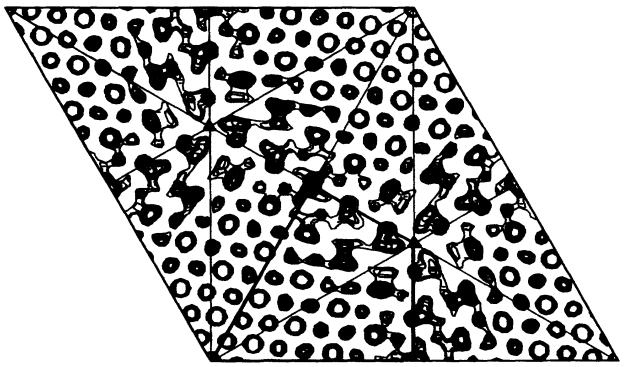

FIG. 3. Experimental Patterson map in the whole reconstructed unit cell. Lines are only guides to locate the threefold axes and the centered twofold axis of the Patterson $p6$ symmetry. The asymmetric unit cell of the Patterson map is delimited by bold lines.

plane atomic positions. The in-plane Debye-Waller factor was fixed at 0.5 $Å^2$ for all atoms, and all possible variants were included in the calculation. The only acceptable model ($\chi^2 = 1.2$) was obtained for the structure shown in Fig. 5, composed of two planes of Al atoms. Removing or adding an Al atom to the unit cell strongly increased the $\chi^2$ value, as did replacing an Al atom by an O atom except within the domain wall. There is evidence for occupancy disorder in the domain walls, because the $\chi^2$ value remains practically constant or even improves by assigning partial occupancies to some atoms within these walls. However, there are not enough data to accurately determine these partial occupancies. The calculated structure factors are compared to the experimental ones in Fig. 1.

The reconstructed structure can be interpreted as a tiling of domains bearing a close resemblance to that of two metal Al(111) planes separated by a hexagonal network of domain walls. In the framework of rotational epitaxy, it has to be compared with that of the parent phase (Fig. 3). These two structures actually differ appreciably.

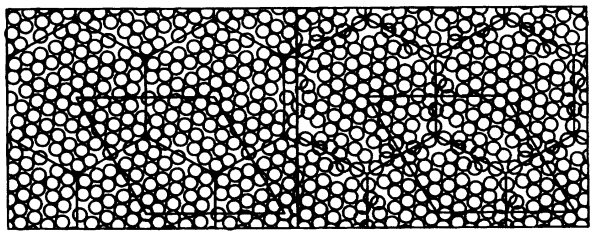


FIG. 4. Several domains of the projected atomic structure of the $(\sqrt{31} \times \sqrt{31})R9°$ reconstruction, where the unit cells as well as domain walls are drawn. The two constituting Al planes are shown separately, with evidence of one being much better ordered than the other. Numerical relaxation has shown that the ordered layer could be associated to the second layer, and the more disordered one to the layer adjacent to the substrate.

In the middle of domains, the overlayers are well ordered, but with a lattice parameter very close to that of metallic Al (expansion of 4% with respect to the registered state) and a small rotation (~1.4° with respect to the $R$ state) with the epitaxial relationships: $(111)Al/(0001)Al_2O_3$ and $[\bar{1}10]Al/(R1.4°)[11\bar{2}0]Al_2O_3$. Both this rotation and expansion are much smaller than that of the parent phase. In addition, in the domain walls, large expansion and rotation, and even loss of honeycomb network topology occur. These large differences are expected [10,11] when the substrate potential is strong enough to favor an intermediate structure between the physisorption case where the main effect is a rotation with weak static distortion waves (SDW) and the strong chemisorption case where nonrotated, registered structures with a 2D network of misfit dislocations are favorable. In the intermediate case, for particular ratios of longitudinal versus transverse stiffness, large SDW are present, with remaining rotations, expansions, and nonlinear (dislocation-type) distortions. The observation of compressed zones (with respect to the parent phase) in near registry separated by narrow domain walls with strong disorder suggests that the substrate potential is strong. This strong substrate potential is responsible for the overlayer to be *commensurate,* since commensurate structures with small CSL are energetically favorable [13] compared to incommensurate structures: they "lock in" the layer as a result of the stabilizing effect of atoms in high-symmetry sites.

Recent theoretical calculations [3] predict that the $\alpha$-$Al_2O_3(0001)$ surface is terminated by an Al layer with $\frac{1}{3}$ compact packing. Hence, starting from the surface, the successive planes are Al-O-Al-Al-O-Al-Al-O.... Removing the two last O planes would thus leave five Al layers with $\frac{1}{3}$ compact packing occupancy at the surface, and hence a filling ratio of $\frac{5}{3} = 1.67$ with respect to the compact commensurate packing, which is almost identical to the observed one, of $157/(3 \times 31) = 1.69$. We then suggest that the reconstruction is obtained after evaporation of the two upper oxygen layers of the unreconstructed surface. However, why just two oxygen layers could evaporate from the surface is still not clear to us. The physical origin of the ~4% expansion in the domains is clear, since the overlayer is very close to bulk Al and registry. The origin of the rotation and domain wall network is more complicated. We believe that the observed structure could be interpreted in the spirit of rotational epitaxy with nonlinear distortions. However, whereas the atomic honeycomb topology is preserved in one of the two Al layers, it is not preserved in the other (Fig. 5). Therefore, none of the existing models of rotational epitaxy [10–14] is applicable in the explanation of the observed reconstruction. A detailed investigation of the interfacial energy requires extensive atomic relaxations where the effect of commensurateness is fully taken into account. A minimum-energy numerical simulation of the two Al planes, interacting with each other and

with the substrate via a Lennard-Jones potential [15] was performed. The initial structure was composed of two CSL unit cells of the parent phase containing 304 Al atoms. Additional atoms were allowed to fill possible holes appearing in the domain walls as a result of relaxation. The relaxed structure was very similar to the experimental one. However, the comparison of experimental and simulated diffraction patterns gives evidence (Fig. 6) of a stronger experimental disorder than expected from the simulations on only two reconstructed unit cells. The numerical relaxation shows that the Al layer closer to the substrate is strongly disordered, in particular, in the region of domain walls, whereas ordering of the second layer is much more regular. The first layer is subject to strong commensurate (but not in registry) potential of the substrate whereas the influence of this potential on the second layer is much weaker. The simulation also shows that in the walls, there are many possible metastable positions. Therefore we expect some occupancy disorder in the walls.

We now discuss the atomic structure determined by GIXD in view of the available results of other surface studies of the $\sqrt{31}$ reconstruction. With regard to the composition, the earlier studies [4,5] already pointed out that the reconstruction is oxygen deficient and limited to one or two atomic layer(s). XPS investigations [4,6] also show intermediate oxidation states of surface aluminum atoms. The surface band gap was also found to be reduced on the reconstructed surface [6,16], which is expected from an Al enriched surface. The fact that this Al terminated surface does not quickly oxidize in alumina when exposed to air at room temperature is probably due to a kinetic limitation, since when exposed to $O_2$ partial pressure, the reconstruction disappears only when heating above 1000 °C [4], as confirmed on our sample.

The atomic structure determined by GIXD also sheds some light on many results of growth and irradiation experiments. It was recently found that $\alpha$-$Al_2O_3$(0001) can be epitaxially grown on top of Al(111) [17], and that an epitaxial Al(111) buried single-crystalline layer in mesotaxy can be formed by high-dose Al ions implantation into $\alpha$-$Al_2O_3$(0001) [18]. In all cases, as well as when depositing other fcc metals like Cu on the $\alpha$-$Al_2O_3$(0001) surface [19], the epitaxial relationships are identical to those of the two reconstructed Al(111) planes. More interestingly, a $\sqrt{31}$ reconstruction is observed [4,20] during the first stage of Al deposition [between 0.4 and 2.5 Al(111) monolayer coverage] on a $\alpha$-$Al_2O_3$(0001) surface with $(1 \times 1)$ structure, followed by Al(111) domain growth for larger coverage. Thus, a fundamental question is open concerning the process and dynamics of this reconstruction formation by different routes: reduction or Al deposition, which could be assessed by future *in situ* surface x-ray diffraction experiments.

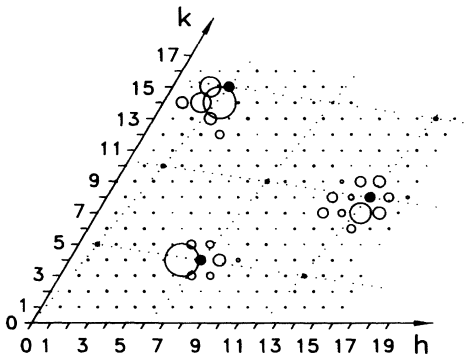


FIG. 5. Diffraction pattern of the simulated overlayer structure, with 154 Al atoms in the reconstructed unit cell. For details, see Fig. 1.

We are greatly indebted to J. Villain for many fruitful discussions. We would like to thank M. Gautier and J. P. Duraud for valuable discussions and for use of their UHV chamber for sample preparation. I. V. thanks the CEA/DRFMC for hospitality and the European Union for financial support.

[1] P. W. Tasker, Adv. Ceram. **10**, 176 (1984).
[2] J. Guo, D. E. Ellis, and D. J. Lam, Phys. Rev. B **45**, 13 647 (1992).
[3] I. Manassidis, A. De Vita, and M. J. Gillan, Surf. Sci. Lett. **285**, L517 (1993).
[4] T. M. French and G. A. Somarjai, J. Phys. Chem. **74**, 12 (1970).
[5] S. Baik, D. E. Fowler, J. M. Blakeley, R. Raj, J. Am. Ceram. Soc. **68**, 281 (1985).
[6] M. Gautier, J. P. Duraud, L. Pham Van, and M. J. Guittet, Surf. Sci. **250**, 71 (1991).
[7] M. Gautier, J. P. Duraud, and L. Pham Van, Surf. Sci. Lett. **249**, L327 (1991).
[8] I. K. Robinson and D. J. Tweet, Rep. Prog. Phys. **55**, 599 (1992).
[9] Y. Kim and T. Hsu, Surf. Sci. **258**, 131 (1991).
[10] A. D. Novaco and J. P. McTague, Phys. Rev. Lett. **38**, 1286 (1977); J. P. McTague and A. D. Novaco, Phys. Rev. B **19**, 5299 (1979).
[11] H. Shiba, J. Phys. Soc. Jpn. **46**, 1852 (1979); **48**, 211 (1980).
[12] Two variants, related by symmetry with respect to the center of the unit cell, result from the lowering of the surface symmetry from sixfold to threefold.
[13] C. R. Fuselier, J. C. Raich, and N. S. Gillis, Surf. Sci. **92**, 667 (1980).
[14] J. Villain, Phys. Rev. Lett. **41**, 36 (1978).
[15] I. Vilfan, J. Villain, and F. Lançon (to be published).
[16] E. Gillet and B. Ealet, Surf. Sci. **273**, 427 (1992).
[17] P. Moller and J. Guo, Thin Solid Films **201**, 267 (1991).
[18] H. Hirayama, G. H. Takaoka, H. Usui, and I. Yamada, Nucl. Instrum. Methods Phys. Res., Sect. B **59/60**, 207 (1991).
[19] M. Ohkubo, N. Suzuki, and T. Hioki, Appl. Phys. Lett. **56**, 2631 (1990).
[20] M. Vermeersch, R. Sporken, Ph. Lambin, and R. Caudano, Surf. Sci. **235**, 5 (1990).